Beam collimation and transport of quasineutral laser-accelerated protons by a solenoid field

Article · February 2010

DOI: 10.1063/1.3299391

12 authors, including:

Knut Michel
TRUMPF Scientific Lasers GmbH + Co. KG
85 PUBLICATIONS **1,715** CITATIONS
SEE PROFILE

Ina Schubert
GSI Helmholtzzentrum für Schwerionenforschung
35 PUBLICATIONS **693** CITATIONS
SEE PROFILE

Vincent Bagnoud
GSI Helmholtzzentrum für Schwerionenforschung
207 PUBLICATIONS **3,460** CITATIONS
SEE PROFILE

Marc M. Günther
GSI Helmholtzzentrum für Schwerionenforschung
43 PUBLICATIONS **558** CITATIONS
SEE PROFILE

Beam collimation and transport of quasineutral laser-accelerated protons by a solenoid field

K. Harres, I. Alber, A. Tauschwitz, V. Bagnoud, H. Daido, M. Günther, F. Nürnberg, A. Otten, M. Schollmeier, J. Schütrumpf, M. Tampo, and M. Roth

Citation: Phys. Plasmas **17**, 023107 (2010); doi: 10.1063/1.3299391
View online: http://dx.doi.org/10.1063/1.3299391
View Table of Contents: http://aip.scitation.org/toc/php/17/2
Published by the American Institute of Physics

Beam collimation and transport of quasineutral laser-accelerated protons by a solenoid field

K. Harres,[1] I. Alber,[1] A. Tauschwitz,[2] V. Bagnoud,[2] H. Daido,[3] M. Günther,[1] F. Nürnberg,[1] A. Otten,[1] M. Schollmeier,[4] J. Schütrumpf,[1] M. Tampo,[3] and M. Roth[1]
[1]*Institut für Kernphysik, Technische Universität Darmstadt, Schlossgartenstraße 9, 64289 Darmstadt, Germany*
[2]*Plasmaphysik and PHELIX, GSI-Helmholtzzentrum für Schwerionenforschung GmbH, Planckstrasse 1, 64291 Darmstadt, Germany*
[3]*Photo Medical Research Center, JAEA, 8-1 Umemidai, Kizugawa City, Kyoto 619-0215, Japan*
[4]*Sandia National Laboratories, Albuquerque, New Mexico 87185, USA*

(Received 11 December 2009; accepted 5 January 2010; published online 12 February 2010)

This article reports about controlling laser-accelerated proton beams with respect to beam divergence and energy. The particles are captured by a pulsed high field solenoid with a magnetic field strength of 8.6 T directly behind a flat target foil that is irradiated by a high intensity laser pulse. Proton beams with energies around 2.3 MeV and particle numbers of 10^{12} could be collimated and transported over a distance of more than 300 mm. In contrast to the protons the comoving electrons are strongly deflected by the solenoid field. They propagate at a submillimeter gyroradius around the solenoid's axis which could be experimentally verified. The originated high flux electron beam produces a high space charge resulting in a stronger focusing of the proton beam than expected by tracking results. Leadoff particle-in-cell simulations show qualitatively that this effect is caused by space charge attraction due to the comoving electrons. The collimation and transport of laser-accelerated protons is the first step to provide these unique beams for further applications such as postacceleration by conventional accelerator structures. © *2010 American Institute of Physics*. [doi:10.1063/1.3299391]

I. INTRODUCTION

Since the first observation of laser-accelerated ions in 2000 (Ref. 1), these beams have attracted a lot of interest due to their unique beam parameters and have triggered an extensive discussion about their possible applications. The ideas range from new diagnostic techniques for short pulse phenomena,[2] the modification of material parameters,[3] ion beam radiography,[4] and applications in energy research (e.g., the "fast ignitor" in the inertial fusion context)[5] up to medical treatment issues.[6]

Experimentally, highest beam fluxes[7] and ultralow emittances[8] were observed, which exceed the quality of ion beams accelerated by conventional accelerator structures in orders of magnitude. Still the main drawbacks of laser-accelerated ions and in particular, protons are the exponential energy spectrum and the large envelope divergence of the beam.[9] Different techniques have been developed to modify the energy distribution to produce a more monoenergetic beam. Therefore special targets were created with thin proton or carbon layers on the rear side,[10,11] as well as deuterated droplets.[12] Besides, there have been attempts to reduce the initial divergence of the beams by ballistic focusing with the help of curved targets in a hemispherical shape,[3] resulting in a beam focus in a distance of the diameter of the sphere from the laser focus. In a different experiment a laser-triggered microlens was used to select a small energy interval and to focus down the protons with these specific energies to a millimeter spot 70 cm from the target.[13] This setup suffers from its complexity since two synchronized high intensity laser beams are required. A much simpler attempt in the field of controlling laser-accelerated protons was carried out in 2008 by Schollmeier *et al.*[14] They used permanent magnet quadrupoles for the guidance of the protons at particle energies of 14 MeV. A focus of only (286×176) μm could be reached with a flux increase in comparison with an unfocused beam of a factor of 75. The quadrupoles had a large magnetic field gradient of 500 T/m to control protons at an energy of 14 MeV. This high field gradient defines a quadrupole design with a small open aperture of only 5 mm, which results in the loss of 99.9% of the protons during the transmission through the quadrupole doublet. To avoid such strong particle losses caused by the focusing devices we have established an alternative to control the transport of laser-accelerated protons that uses a pulsed high field solenoid to collimate the beam directly behind the target foil. This solenoid runs at a magnetic field strength of 8.6 T and has an open aperture of 44 mm in diameter to catch nearly the full beam at a proton energy of 2.5 MeV. The coil of the solenoid consists of a brass helix originally designed as a Faraday rotator. The design was modified to fit the requirements of the new application as a focusing device, especially to enable the operation under high mechanical stress. The magnetic pressure, p, induced in a pulsed solenoid is given by $p=B^2/2\mu_0$. This means for the used device the magnetic pressure inside the coil reached nearly 30 MPa at a magnetic field strength of 8.6 T, which was the working level during the experiment. Nevertheless, the solenoid was successfully tested up to a magnetic field strength of 15 T that equals 90 MPa magnetic pressure.

The particle trajectory of a charged particle propagating through the magnetic field of a solenoid is given by

$$\gamma m_0\left(\frac{d\vec{v}_r}{dt}\right) = -q\vec{v}_\Theta \times \vec{B}_z + \gamma m_0 \frac{\vec{v}_\Theta^2}{r}, \quad (1)$$

$$\gamma m_0\left(\frac{d\vec{v}_\Theta}{dt}\right) = -q\vec{v}_z \times \vec{B}_r + \gamma m_0 \vec{v}_r \frac{\vec{v}_\Theta}{r}. \quad (2)$$

Here $\vec{v}_z$, $\vec{v}_r$, and $\vec{v}_\Theta$ are the axial, radial, and rotation velocity of the particle, γ is the relativistic factor, m_0 and q are the mass and the charge of the particle, r is the distance of the position of the particle to the solenoid's axis, and $\vec{B}_z$ and $\vec{B}_r$ are the magnetic field components in axial and radial direction, respectively. Assuming a constant axial velocity $\vec{v}_z$, no radial magnetic field $\vec{B}_r$ inside the solenoid and a small radial velocity $\vec{v}_r$ in comparison with the axial component, the term of the Coriolis force, $\gamma m_0 \vec{v}_r(\vec{v}_\Theta)/r$ can be neglected and therefore the right-hand side of Eq. (2) becomes zero. Hence, the rotation velocity v_Θ inside the solenoid is constant. A charged particle beam gets focused if the Lorentz force, $q\vec{v}_\Theta \times \vec{B}_z$, exceeds the centrifugal force, $\gamma m_0(\vec{v}_\Theta^2)/r$, see Eq. (1). A collimation, i.e., a parallelization of the particle trajectories of a divergent beam is reached if the gained radial velocity to the axis has the same amount as the initial radial component $\vec{v}_r$.

To predict the proton propagation through the solenoid focusing device and to define the final solenoid design, simulations with Computer Simulation Technology (CST) Particle Studio[15] were done. This code is based on the finite volume method used to solve the Maxwell equations. It allows to set up a full three-dimensional model of the experimental device, calculates the electromagnetic fields and also includes a particle tracker as well as a particle-in-cell (PIC) solver that considers space charge effects.

The structure of this article is as follows: Section II describes the setup of the experiment, gives information about the used detectors and about the solenoid. In Sec. III, experimental results of the proton transport by the solenoid are presented. Several simulations were done to calculate the proton propagation through the solenoid, which are shown in Sec. IV, together with a comparison with the experimental results.

II. EXPERIMENTAL SETUP

The experiment was carried out at the Petawatt High Energy Laser for Ion eXperiments (PHELIX) facility at GSI-Helmholtzzentrum für Schwerionenforschung GmbH in Darmstadt, Germany. This laser system holds two different front ends, one nanosecond as well as a femtosecond front end that was used for the described experiment. The laser energy before compression was up to 150 J. At a compressor efficiency of 90% and a parabola reflectivity of around 80% the intensity in the focus with a full width at half maximum of $\pi(12/2\times18/2)$ μm^2 reached 4.5×10^{19} W/cm^2 at a pulse length of 700 fs. This campaign was the first run of the laser system working at high energy and during the first shots laser-accelerated protons with energies exceeding 30 MeV could be observed.

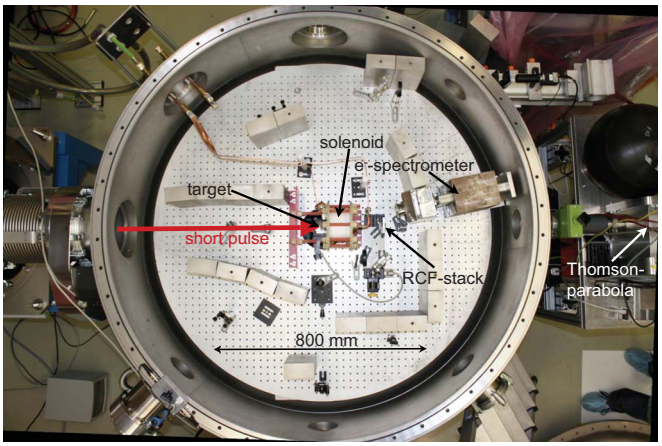

FIG. 1. (Color online) Experimental setup at the target area of PHELIX. The laser enters the target chamber from the left side. The solenoid is placed right behind the target in the middle of the chamber. The produced proton beam is detected by an RCF stack, a magnetic spectrometer and outside the target chamber by a Thomson parabola.

Different diagnostics were used to detect the proton beam. The main diagnostic were calibrated radiochromic films (RCFs),[16] which are sensitive to ionizing radiation and turn blue after exposition. By using the films in a stack configuration, they deliver energy and space resolved data about the proton beam. This is done by a deconvolution of the deposited dose in each RCF layer.[17] Additionally, a Thomson spectrometer[18] was used as well as a magnetic spectrometer that was designed to deliver data about protons, electrons and even positrons at the same time.

The experimental setup is shown in Fig. 1. The laser beam entered the target chamber from the left side and was focused down to the target chamber center where the target was placed at an incidence angle of 0°. The solenoid was mounted in laser propagation direction at a distance of 17 mm to the target. An RCF-stack to detect the proton beam was placed 130 mm behind the solenoid on axis that equals a target-detector distance of 241 mm. The Thomson parabola spectrometer stood outside the target chamber at the incidence angle of the laser. Inside the chamber the magnetic spectrometer was mounted at an angle of 11° to the target rear normal. The targets were thin flat gold foils, with thicknesses between 10 and 50 μm.

As mentioned above the solenoid was tested up to a magnetic field strength of 15 T but was run in the experiment at 8.6 T. The reason for this was that with increasing magnetic field, which is equal to a stronger current applied to the solenoid, an increasing signal on the grounding cable of the solenoid was measured. Figure 2 shows the measured signals of the current going through the solenoid during a test shot in vacuum without the laser [Fig. 2(a)] and at a real shot with the laser during the experiment [Fig. 2(b)]. The red line is the ground signal. For the experiment shot a current of up to 160 A was measured. In addition, the falling slope of the capacitor currents got steeper in comparison with Fig. 2(a). This happened due to the expanding plasma penetrating into the solenoid and creating a short circuit inside the coil resulting in a lower Ohmic resistance and therefore in a lower damp-

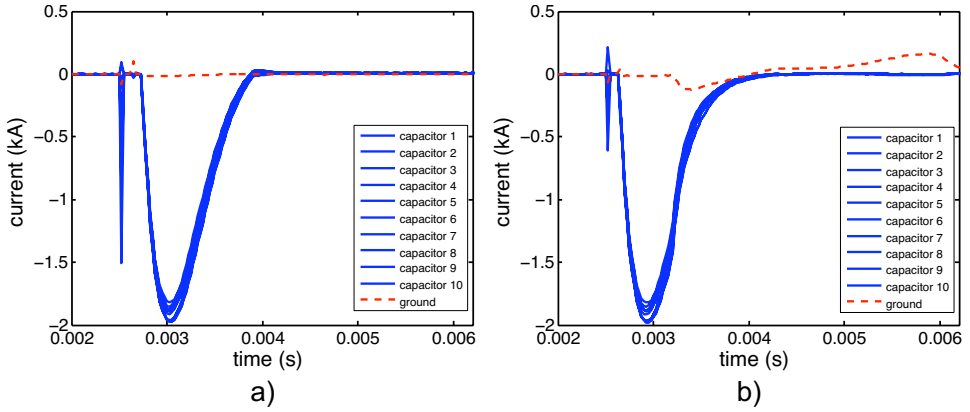

FIG. 2. (Color online) Measured current that was applied to the solenoid. The dashed line shows the ground signal. At a full system shot including the laser, a signal of 160 A was measured starting at the time the laser had hit the target (b). This is caused by the expanding plasma entering the solenoid and hitting the inner wall which leads to arcing. Without the laser hitting the target no signal was measured on the ground (a).

ing of the system. The time at which the ground current appeared perfectly fit with the time when the laser has hit the target. The shift in time between the positions of the maximum current shown in the two graphs is not caused by the short circuit. A different timing was used at the full shot to get a perfect synchronization between maximum magnetic field and laser hitting the target. Although the ground signal is only a small fraction of the total current that is lost due to the short circuit it could be observed that this ground signal got stronger with increasing current and for safety reasons the maximum applied current had to be limited to 19 kA. This equals a magnetic field strength of 8.6 T, which allows to collimate a proton beam of 2.5 MeV particle energy.

III. PROTON AND ELECTRON TRANSPORT

To verify the strong influence of the solenoid on the proton beam propagation, reference shots without the magnetic field were done where the RCF stack was placed at the same position of 241 mm behind the target as in a full system shot including the solenoid. Figure 3 shows three RCF stacks, layers 1–6, after irradiation by the proton beam. The denoted energies belong to protons that are stopped in the specific RCF layers. On the left, Fig. 3(a), the shown RCF stack was placed at a distance of 40 mm behind the target to observe the whole beam. It is known that the laser beam profile is transferred to the accelerated electrons, as well as to the proton beam.[19] Figure 3(b) shows the reference shot at a distance of 241 mm. Due to the strong divergence of the beam (25° half opening angle for protons with energies below 10 MeV) only a few particles are detected by the RCF. At energies higher than 6.0 MeV only a weak proton background is visible due to the fact that the number of protons for these energies is below the RCF detection threshold of 10^8. Layers 1–3 show a kind of a ring structure in the beam. The reason for this could be recirculating electrons that are accelerated several times by the laser, see, e.g., Ref. 20. The slit in the films is needed since a small part of the beam has to propagate further to be detected by the Thomson parabola and the magnetic spectrometer.

In comparison with Figs. 3(a) and 3(b), Fig. 3(c) shows the RCF stack of an experiment where the solenoid was energized to collimate the beam. The RCF stack was placed at the same distance of 241 mm behind the target, which equals a distance of 130 mm from the exit of the solenoid to the detector stack. The magnetic flux density was 8.6 T. As expected from the particle tracking simulations the first RCF at 2.3 MeV proton energy shows a strong signal. The beam diameter is 39 mm in vertical direction and 42 mm in horizontal direction (red circle). A diameter of 40 mm was the result of the CST calculations, but it has to be considered that

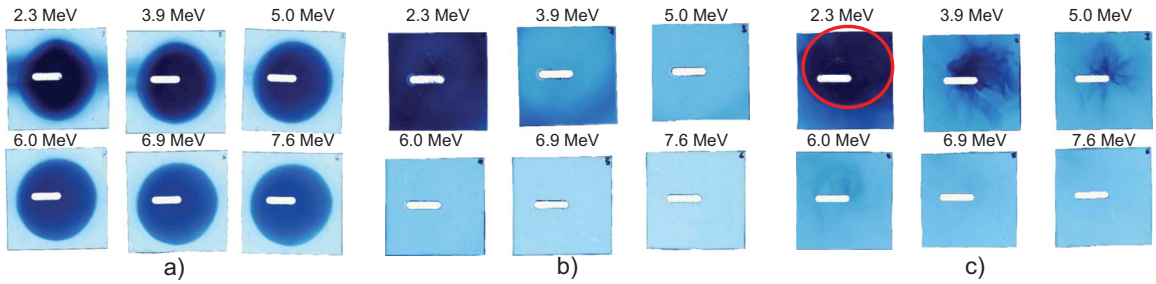

FIG. 3. (Color online) The proton beam measured by RCF at a distance of 40 mm to the target (a) and at a distance of 241 mm (b). The slit in the RCF was necessary so that a part of the beam could propagate further and get detected by the spectrometers. (c) The proton beam measured behind the solenoid at a distance of 241 mm to the target. Due to the collimation a strong proton signal was detected at 2.3 MeV particle energy. The beam size (circle at 2.3 MeV) is 42 mm in the horizontal and 39 mm in the vertical direction. Even for higher energies a clear proton signal could be observed due to the additional focusing effect by the co-moving electrons.

the RCF detects an energy band and not one specific energy, so that higher energies with a larger divergence color the film as well. This dose needs to be subtracted while analyzing the RCF. The beam shape is slightly elliptical as in Fig. 3(a) but not that clear defined. Several modulations can be seen, which will be discussed later.

To characterize the solenoid device its collimation efficiency needs to be compared to different experiments. In addition to the experiment by Schollmeier *et al.*[14] a second experiment using a permanent quadrupole focusing device is described in Ref. 21. In this experiment the collimation of protons with energies of (3.7 ± 0.3) MeV was investigated. The particle losses inside the quadrupole doublet were 25%. Additionally, due to the open aperture of the quadrupoles of 50 mm in diameter and their distance to the target of 150 mm, only protons with a half opening angle of 10° could enter the quadrupole doublet. The envelope divergence of the beam was 20° half opening angle, so that only a small fraction of the beam was captured by the collimation device at all.

A comparison of RCF layer 1 (2.3 MeV proton energy) of Figs. 3(a) and 3(c) by using the radiochromic film imaging spectroscopy (RIS) technique[16] to calculate the total particle numbers shows that in both cases the proton numbers reach 10^{12}. The error estimate for the proton numbers given by RIS is around 20%. The tracking simulations predict that 10% of the initial beam will be stopped inside the solenoid by hitting the inner walls. This means even in a worst-case-scenario, the particle numbers are still above a few times 10^{11}. This is the first time that such an intense laser-accelerated proton beam could be transported over a distance of more than 300 mm.

Besides the detection of a strong signal in the first RCF layer, a second remarkable observation is that not only in the first layer of the RCF stack, shown in Fig. 3(c) but also in layers 2–4 a clear proton signal can be seen. In principle all protons with higher energies will be collimated or focused less than these at exactly 2.5 MeV, so that a larger beam size and only a few particles, as seen in Fig. 3(b), are expected to be measured by layers 2–4. To explain this effect it has to be considered that during the laser-plasma interaction not only protons get accelerated but also electrons with even higher particle numbers than the proton numbers. The energies of the electrons range from tens of MeV down to a few eV.[22] Hence, the transport of the proton beam through the solenoid gets much more complicated since all comoving electrons, i.e., electrons traveling at the same velocities as the protons, pass through the solenoid field at the same time as the proton beam. The light electrons are forced down to the solenoid's axis by the magnetic field building up a non-negligible space charge that attracts the protons. For example, the gyroradius of an electron with an energy of 5 keV at the center of the solenoid at 8.6 T can be calculated to $r_e = \gamma\sqrt{2m_eE}/q_eB \approx 28$ μm. Even protons up to 6 MeV could be detected by the RCF stack, see Fig. 3(c) fourth layer, which shows that even higher energetic protons get affected by this electric field. Not only at a distance of 241 mm to the target but even at a distance of 324 mm clear proton signals in the first four layers could be observed, with similar shape to the ones shown in Fig. 3(c).

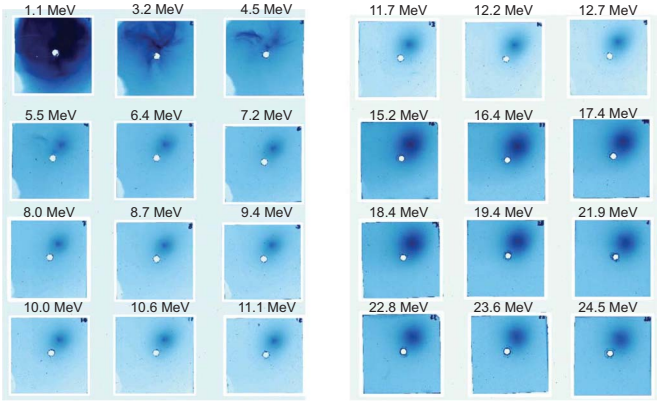

FIG. 4. (Color online) RCF stack after irradiation. Additionally to the proton signal in the first four layers, a well-defined electron signal was measured through the whole RCF stack. In the last nine layers a stronger signal and background intensity of the electron beam can be seen. These layers are a different RCF type with a much higher sensitivity than the ones used in the front of the stack.

The deflection of the protons due to the space charge field arising from the comoving electrons influences the emittance of the proton beam, since electric fields do not preserve the beam emittance. Detailed studies about emittance growth are beyond the scope of this work and will be done in future experiments. In addition, these results have to be compared with the influence of the solenoid's field on the beam emittance caused by chromatic aberrations.[23]

The existence of the electron beam circulating around the solenoid's axis with its gyroradius could be experimentally verified. Figure 4 shows an RCF stack after irradiation that was placed as close to the solenoid as possible at a distance of only 161 mm to the target. Besides the well-known proton signal in the first four layers a second beam was measured throughout the whole RCF stack up to the last layer. The signal stays constant in intensity, therefore it was not generated by protons because of their high stopping power. Instead an electron beam with a particle energy of only 2 MeV (not only the comoving electrons but also higher energetic electrons circulate around the solenoid's axis) can easily penetrate through an RCF stack consisting of 24 layers. In the last nine layers a stronger signal and background intensity of the electron beam can be seen. These layers are a different RCF type with a much higher sensitivity than the ones used in the front of the stack. The electron beam could not be observed in shots where the RCF stack was placed 241 mm or even further away from the target since the electron beam rapidly breaks up behind the solenoid due to the dispersion of the magnetic field lines and due to the Coulomb repulsion of the electrons among each other.

Additionally, strong beam modulations could be seen in the RCF layers when using the solenoid in comparison with a standard laser-proton acceleration without any collimation device. This could originate due to the interaction between electrons and protons inside the solenoid. A second phenomena had strong influence on the beam shape as well. Strong eddy currents were induced in the gold foil by the solenoid

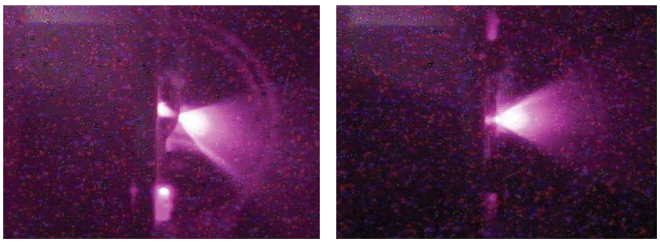

FIG. 5. (Color online) Images of the laser-plasma interaction. Picture (a) shows a shot where the target got bent by the strong magnetic field of the solenoid inducing eddy currents in the target. On the right side (b), a shot without the solenoid firing is shown.

field (950 mT at the target position), which led to a bending of the target. Figure 5 shows two pictures of laser-plasma interactions taken with a digital camera that was mounted outside of the target chamber at an angle of 90° to the target normal. In both pictures the plasma expansion at the front as well as at the rear surface of the target are clearly visible. The strong curvature of the gold foil in Fig. 5(a) is conspicuous. The target was bent up to $18° \pm 1°$. This strong movement of the foil influences the proton acceleration and the collimation in several ways. First of all the target is moved out of the focal plane of the laser by more than the target thickness (20–50 μm), which leads to a drop in the laser intensity and therefore in a change of the proton spectrum. The second point is related to the collimation process. A proton beam that enters the solenoid with an incidence angle of 18° to the solenoids axis cannot be collimated as efficient as at 0°. Lots of particles will hit the inner wall and get lost. CST Particle Studio tracking calculations were done to simulate the effect of a 18° bent target. At an energy of 2.3 MeV 50% of the protons are stopped inside the detector and the intensity maximum of the beam image at the RCF position is moved out of the center by 15 mm. The bending can easily be suppressed by using non conductive targets but insulator material suppresses the electron transport through the target which weakens the laser-ion acceleration.[24] This subject needs further investigations.

IV. SIMULATIONS

The experimentally observed results were checked by leadoff CST Particle Studio PIC simulations, which demonstrate the effect of electrostatic attraction inside the solenoid between electrons and protons. The simulations only deliver qualitative results about this very complex system. An accurate determination of the particle propagation from the target position with a particle source size of only a few hundred microns to the position of the RCF detector 130 mm behind the solenoid is not realizable since the calculation mesh of CST Particle Studio cannot be adapted to such a system at all and the particle numbers that are linked to the mesh configuration are far too low. The mesh size is too coarse at the target and too fine inside the solenoid after the beam has diverged. Nevertheless, the PIC simulations can approximately show the interaction between electrons and protons in the solenoid and the results fit the experimental observations.

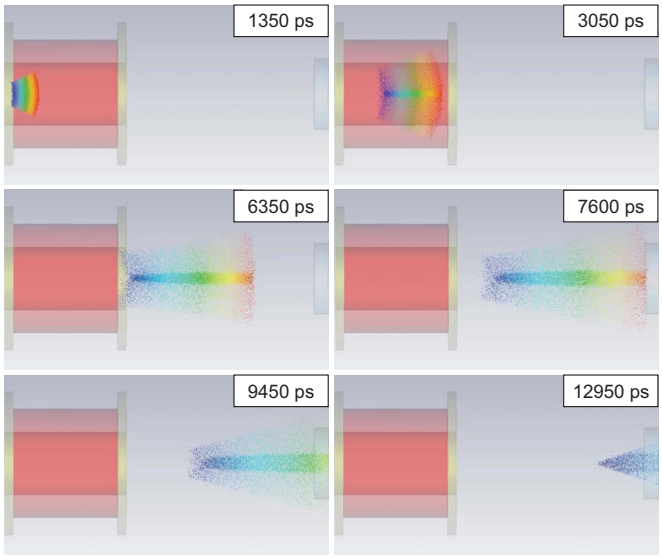

FIG. 6. (Color online) Propagation of the proton beam through the solenoid (left side) to the RCF detector (right side) at different time steps. The strong aggregation of the proton beam due to the electron's space charge is clearly visible. The positions of the particles indicate their energy from the lowest value (1 MeV, in the rear of the pulse) to the highest one (5 MeV, in the front of the pulse).

All calculations were done at the same parameter settings. The particle density, i.e., the number of electrons and protons, was adjusted to the mesh and was 8255 particles per excitation time step and per species. The excitation signal that defines the time how long new particles were created was 0.8 ps. This resulted in a total particle number of 49 530 in the beam. The emission models of the particle beams were given by Gaussian distributions with a total bunch charge of 10^{-7} C, which equals 6×10^{11} real particles for each species. The spatial resolution of the used mesh was 100 μm in all directions. The time step width was 407 fs.

The particle tracking simulations without considering any space charges already show that the electrons are forced down to the solenoid's axis by the strong magnetic field directly at the target position (the magnetic field strength at the target in a distance of 17 mm to the solenoid is around 0.95 T) that leads to a negative space charge accumulation around the axis. The electrostatic attraction of the strongly collimated electron beam on the protons changes the beam profile quite significantly.

The time evolution of the propagating protons from 1350 to 12 950 ps after the laser has hit the target is shown in Fig. 6. The electrons are not plotted in this figure. The proton energies are between 1 MeV (blue dots) and 5 MeV (red dots). The proton beam has entered the solenoid on the left side of the picture and propagates to the right until it is stopped in the detector stack. A strong aggregation of the beam around the solenoid's axis was found. At later time steps the aggregation of the beam smears out linked to the decrease in the field strength with increasing distance to the solenoid. This happens due to the break up of the strongly collimated electron beam. The electrons still follow the magnetic field lines that are not parallel anymore but are oriented outwards, away from the solenoid's axis.

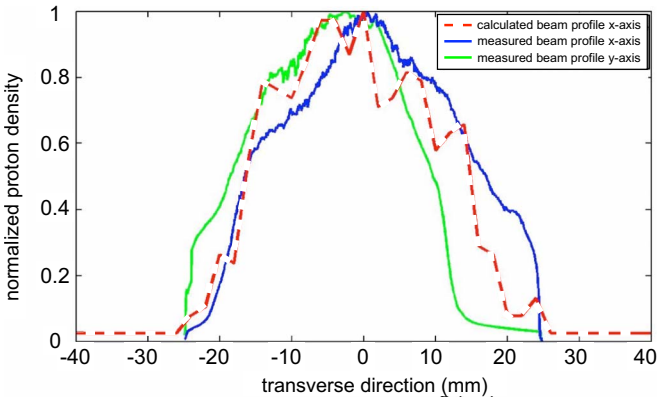

FIG. 7. (Color online) Experimental (solid lines) and theoretical (dashed line) beam profiles of 2.3 MeV protons at the RCF position 241 mm behind the target.

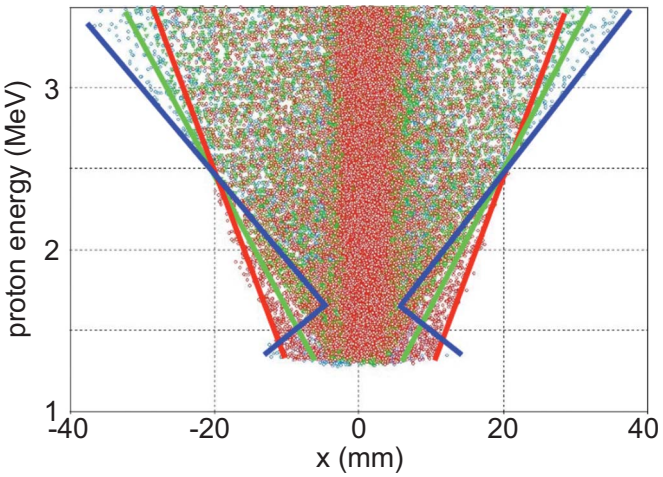

FIG. 8. (Color online) Proton energy vs transverse space coordinate perpendicular to the beam propagation direction. The protons are shown for three different time steps after the laser had hit the target—7.6 ns, 9.45 ns, and 12.95 ns. The solid lines show the individual beam envelopes–smallest beam size at 7.6 ns to largest beam size at 12.95 ns. The beam size stays constant close to 2.5 MeV (intersection point of all three envelopes) which means that these protons were parallelized by the solenoid. See the text for more details.

To illustrate the change of the beam divergence in time Fig. 7 shows the energy of the protons versus the transverse space coordinate x. It is plotted for three different time steps 7600 ps (red dots), 9450 ps (green dots), and 12 950 ps (blue dots). The three solid lines highlight the beam envelopes. The proton beam is divergent for particles with energies greater than 2.5 MeV, which can be seen by the larger opening angle for the later time steps. A collimated beam is reached at the energy of around 2.5 MeV where all three envelopes cross. No change in divergence can be observed during time evolution at this energy. At smaller energies the divergence is getting smaller with time. The exception are particles with energies lower than 1.7 MeV. A strong bend in the envelope of the latest time step (blue line) exists. At this point particles with lower energies than 1.7 MeV already got through the focus and diverge again. The strong aggregation of the proton beam on axis is quite obvious as well and it is getting weaker for later time steps.

A comparison between experimental and simulation results are given in Fig. 8. It shows line out plots of the beam profile of the first RCF layer of Fig. 3(c) in x-direction and y-direction (transverse to the beam propagation direction) together with the simulated line out by CST Particle Studio. The y-direction of the simulation was skipped since it looks nearly the same as the x-direction. A very good agreement in the beam profiles was observed. For each data point on the transverse direction all data points on the perpendicular transverse direction were summed up to create the line out. The proton density for all data was scaled to one since CST Particle Studio does not support the calculation of 10^{12} particles at all. However, the total beam charge was set to the same level as in the experiment, so that the influence of the magnetic field on the beam is the same in the simulation as in the experiment. The blue curve has a weak peak around the center of the beam that resulted due to the proton density modulations.

Detailed calculations of the propagation process of laser-accelerated protons and their comoving electrons through a high field solenoid device have started in our group using the Warp code.[25] First results that support the above described observations can be found in Ref. 26.

V. CONCLUSION

In this article we have shown that the collimation of a laser-accelerated proton beam by a pulsed high field solenoid is possible and leads to good results in terms of collimation efficiencies. 10^{12} particles could be caught and transported by the solenoid. The steadiness of the proton beam after collimation could be proven up to a distance of 324 mm from the target position. Inside the solenoid strong space charge effects occurred due to the comoving electrons that are forced to circulate around the solenoid's axis at their gyroradius by the strong magnetic field, leading to a proton beam aggregation around the axis. This resulted in a stronger focusing of the beam so that even higher energies than the expected 2.3 MeV could be observed by the RCF. The operation of the solenoid was limited by safety issues so that the magnetic field strength was limited to 8.6 T, which equals a current of 19 kA. This problem will be solved for future experiments as well as the effect that the target got bent by the induced eddy currents. Nevertheless at the investigated proton energy of 2.5 MeV the experimental and computational results match very well.

ACKNOWLEDGMENTS

The authors would like to thank the divisions of PHELIX and plasma physics at GSI for their excellent support. This work was supported by Bundesministerium für Bildung und Forschung (BMBF), support code 06 DA 122 I. Sandia is a multiprogram laboratory operated by Sandia Corporation, a Lockheed Martin Co., for the United States Department of Energy's National Nuclear Security Administration under Contract No. DE-AC04-94AL85000.

[1] R. A. Snavely, M. H. Key, S. P. Hatchett, T. E. Cowan, M. Roth, T. W. Phillips, M. A. Stoyer, E. A. Henry, T. C. Sangster, M. S. Singh, S. C. Wilks, A. MacKinnon, A. Offenberger, D. M. Pennington, K. Yasuike, A.

B. Langdon, B. F. Lasinski, J. Johnson, M. D. Perry, and E. M. Campbell, Phys. Rev. Lett. **85**, 2945 (2000).
[2]M. Borghesi, A. Schiavi, D. H. Campbell, M. G. Haines, O. Willi, A. J. MacKinnon, L. A. Gizzi, M. Galimberti, R. J. Clarke, and H. Ruhl, Plasma Phys. Controlled Fusion **43**, 267 (2001).
[3]P. K. Patel, A. J. Mackinnon, M. H. Key, T. E. Cowan, M. E. Foord, M. Allen, D. F. Price, H. Ruhl, P. T. Springer, and R. Stephens, Phys. Rev. Lett. **91**, 125004 (2003).
[4]A. J. Mackinnon, P. K. Patel, M. Borghesi, R. C. Clarke, R. R. Freeman, H. Habara, S. P. Hatchett, D. Hey, D. G. Hicks, S. Kar, M. H. Key, J. A. King, K. Lancaster, D. Neely, A. Nikkro, P. A. Norreys, M. M. Notley, T. W. Phillips, L. Romagnani, R. A. Snavely, R. B. Stephens, and R. P. J. Town, Phys. Rev. Lett. **97**, 045001 (2006).
[5]M. Roth, T. E. Cowan, M. H. Key, S. P. Hatchett, C. Brown, W. Fountain, J. Johnson, D. M. Pennington, R. A. Snavely, S. C. Wilks, K. Yasuike, H. Ruhl, F. Pegoraro, S. V. Bulanov, E. M. Campbell, M. D. Perry, and H. Powell, Phys. Rev. Lett. **86**, 436 (2001).
[6]S. V. Bulanov and V. S. Khoroshkov, Plasma Phys. Rep. **28**, 453 (2002).
[7]M. A. Stoyer, T. C. Sangster, E. A. Henry, M. D. Cable, T. E. Cowan, S. P. Hatchett, M. H. Key, M. J. Moran, D. M. Pennington, M. D. Perry, T. W. Phillips, M. S. Singh, R. A. Snavely, M. Tabak, and S. C. Wilks, Rev. Sci. Instrum. **72**, 767 (2001).
[8]T. E. Cowan, J. Fuchs, H. Ruhl, A. Kemp, P. Audebert, M. Roth, R. Stephens, I. Barton, A. Blazevic, E. Brambrink, J. Cobble, J. Fernandez, J.-C. Gauthier, M. Geissel, M. Hegelich, J. Kaae, S. Karsch, G. P. Le Sage, S. Letzring, M. Manclossi, S. Meyroneinc, A. Newkirk, H. Pepin, and N. Renard-LeGalloudec, Phys. Rev. Lett. **92**, 204801 (2004).
[9]M. Zepf, E. L. Clark, F. N. Beg, R. J. Clarke, A. E. Dangor, A. Gopal, K. Krushelnick, P. A. Norreys, M. Tatarakis, U. Wagner, and M. S. Wei, Phys. Rev. Lett. **90**, 064801 (2003).
[10]H. Schwoerer, S. Pfotenhauer, O. Jäckel, K.-U. Amthor, B. Liesfeld, W. Ziegler, R. Sauerbrey, K. W. D. Ledingham, and T. Esirkepov, Nature (London) **439**, 445 (2006).
[11]B. M. Hegelich, B. J. Albright, J. Cobble, K. Flippo, S. Letzring, M. Paffett, H. Ruhl, J. Schreiber, R. K. Schulze, and J. C. Fernandez, Nature (London) **439**, 441 (2006).
[12]S. Ter-Avetisyan, M. Schnürer, P. V. Nickles, M. Kalashnikov, E. Risse, T. Sokollik, W. Sandner, A. Andreev, and V. Tikhonchuk, Phys. Rev. Lett. **96**, 145006 (2006).
[13]T. Toncian, M. Borghesi, J. Fuchs, E. d'Humieres, P. Antici, P. Audebert, E. Brambrink, C. A. Cecchetti, A. Pipahl, L. Romagnani, and O. Willi, Science **312**, 410 (2006).
[14]M. Schollmeier, S. Becker, M. Geißel, K. A. Flippo, A. Blazevic, S. A. Gaillard, D. C. Gautier, F. Grüner, K. Harres, M. Kimmel, F. Nürnberg, P. Rambo, U. Schramm, J. Schreiber, J. Schütrumpf, J. Schwarz, N. A. Tahir, B. Atherton, D. Habs, B. M. Hegelich, and M. Roth, Phys. Rev. Lett. **101**, 055004 (2008).
[15]T. Weiland, Int. J. Numer. Model. **9**, 295 (1996).
[16]W. L. McLaughlin, M. Al-Sheikhly, D. F. Lewis, A. Kovacs, and L. Wojnarovits, in *Irradiation of Polymers*, ACS Symposium Series, edited by R. L. Clough and S. W. Shalaby (American Chemical Society, Washington, D.C., 1996), Chap. 11.
[17]F. Nürnberg, M. Schollmeier, E. Brambrink, A. Blazevic, D. C. Carroll, K. Flippo, D. C. Gautier, M. Geißel, K. Harres, B. M. Hegelich, O. Lundh, K. Markey, P. McKenna, D. Neely, J. Schreiber, and M. Roth, Rev. Sci. Instrum. **80**, 033301 (2009).
[18]K. Harres, M. Schollmeier, E. Brambrink, P. Audebert, A. Blazevic, K. Flippo, D. C. Gautier, M. Geiel, B. M. Hegelich, F. Nürnberg, J. Schreiber, H. Wahl, and M. Roth, Rev. Sci. Instrum. **79**, 093368 (2008).
[19]M. Schollmeier, K. Harres, F. Nürnberg, A. Blazevic, P. Audebert, E. Brambrink, J. C. Fernandez, K. A. Flippo, D. C. Gautier, M. Geißel, B. M. Hegelich, J. Schreiber, and M. Roth, Phys. Plasmas **15**, 053101 (2008).
[20]A. J. Mackinnon, Y. Sentoku, P. K. Patel, D. W. Price, S. Hatchett, M. H. Key, C. Andersen, R. Snavely, and R. R. Freeman, Phys. Rev. Lett. **88**, 215006 (2002).
[21]S. Ter-Avetisyan, M. Schnürer, R. Polster, P. V. Nickles, and W. Sandner, Laser Part. Beams **26**, 637 (2008).
[22]T. E. Cowan, M. Roth, J. Johnson, C. Brown, M. Christl, W. Fountain, S. Hatchett, E. A. Henry, A. W. Hunt, M. H. Key, A. MacKinnon, T. Parnell, D. M. Pennington, M. D. Perry, T. W. Phillips, T. C. Sangster, M. Singh, R. Snavely, M. Stoyer, Y. Takahashi, S. C. Wilks, and K. Yasuike, Nucl. Instrum. Methods Phys. Res. A **455**, 130 (2000).
[23]I. Hofmann, A. Orzhekhovskaya, S. Yaramyshev, I. Alber, K. Harres, and M. Roth, Proceedings of the 11th International Conference on Heavy Ion Accelerator Technology (HIAT09) (to be published).
[24]M. Roth, A. Blazevic, M. Geissel, T. Schlegel, T. E. Cowan, M. Allen, J.-C. Gauthier, P. Audebert, J. Fuchs, J. Meyer-ter-Vehn, M. Hegelich, S. Karsch, and A. Pukhov, Phys. Rev. ST Accel. Beams **5**, 061301 (2002).
[25]D. P. Grote, A. Friedman, J.-L. Vay, and I. Haber, AIP Conf. Proc. **749**, 55 (2005).
[26]F. Nürnberg, I. Alber, A. Friedman, D. P. Grote, K. Harres, B. G. Logan, M. Schollmeier, and M. Roth, "WARP simulations for capture and control of laser-accelerated proton beams" in Proceedings of the Sixth International Conference on Inertial Fusion Sciences and Applications (IFSA2009), J. Phys.: Conf. Ser. (to be published).